Biomaterials 35 (2014) 3516–3526

Contents lists available at ScienceDirect

Biomaterials

journal homepage: www.elsevier.com/locate/biomaterials

Stemness and transdifferentiation of adipose-derived stem cells using L-ascorbic acid 2-phosphate-induced cell sheet formation

Jiashing Yu [a,1], Yuan-Kun Tu [b,1], Yueh-Bih Tang [c], Nai-Chen Cheng [c,d,*]

[a] Department of Chemical Engineering, College of Engineering, National Taiwan University, Taipei, Taiwan
[b] Department of Orthopedics, E-Da Hospital/I-Shou University, Kaohsiung, Taiwan
[c] Department of Surgery, National Taiwan University Hospital and College of Medicine, Taipei, Taiwan
[d] Research Center for Developmental Biology and Regenerative Medicine, National Taiwan University, Taipei, Taiwan

ARTICLE INFO

Article history:
Received 19 December 2013
Accepted 8 January 2014
Available online 24 January 2014

Keywords:
Adipose-derived stem cells
Stemness
Differentiation
Cell sheet
Collagen
Wound healing

ABSTRACT

Cell sheet technology has emerged as an important tissue engineering approach. Adipose-derived stem cells (ASCs) have valuable applications in regenerative medicine, but their stemness and differentiation capabilities in the cell sheet format have not been well investigated. In this study, we found that L-ascorbate 2-phosphate (A2-P), a stable form of ascorbic acid, significantly enhanced ASC proliferation and induced ASC sheet fabrication in 7 days with abundant extracellular matrix deposition. Importantly, A2-P treatment significantly enhanced expression of pluripotent markers Sox-2, Oct-4 and Nanog, but treating ASCs with antioxidants other than A2-P revealed no stemness enhancement. Moreover, ASC treatment with A2-P and a collagen synthesis inhibitor, L-2-azetidine carboxylic acid or cis-4-hydroxy-D-proline, significantly inhibited the A2-P-enhanced expression of stemness markers. These findings demonstrated that A2-P enhances stemness of ASCs through collagen synthesis and cell sheet formation. We also showed that A2-P-stimulated collagen synthesis in ASCs may be mediated through ERK1/2 pathway. By culturing the ASC sheets in proper induction media, ASC transdifferentiation capabilities into neuron and hepatocyte-like cells were significantly enhanced after cell sheet formation, while adipogenic and osteogenic differentiation capacities were still maintained. Using a murine model of healing-impaired cutaneous wound, faster wound healing was noted in the group that received ASC sheet treatment, and we observed significantly more engrafted ASCs with evidence of differentiation toward endothelial and epidermal lineages in the cutaneous wound tissue. Therefore, A2-P-mediated ASC sheet formation enhanced ASC stemness and transdifferentiation capabilities, thereby representing a promising approach for applications in regenerative medicine.

1. Introduction

Mesenchymal stem cells (MSCs), which are capable of self-renewal and multi-lineage differentiation, have been regarded to have great potential for their application in regenerative medicine. As a potential autologous cell source, the use of MSCs circumvents the complications associated with allogeneic transplantation. Moreover, clinical application of MSCs exhibits virtually no ethical issue that encountered with the use of embryonic stem cells. Among the various sources of MSCs, adipose-derived stem cell (ASC) represents an abundant source of multipotent adult stem cells that are easily obtained from subcutaneous adipose tissue via minimally invasive procedures, such as liposuction [1,2]. As many as 1% of adipose cells are estimated to be stem cells, compared to the 0.001–0.002% found in bone marrow, currently a common source of MSCs [3]. In addition to the ability of self-renewal, ASCs can differentiate into multiple lineages when cultivated under lineage-specific conditions, including osteogenic, adipogenic, and chondrogenic lineages [4]. This ability, together with their easy accessibility and low donor site morbidity, has made ASCs good candidates for a broad range of cell-based therapeutics.

Cell sheet technology has been applied to enhance the regenerative effects of tissue-engineered products in recent years [5,6]. With a cell sheet approach, cell-to-cell connections are not disrupted and cells are harvested as a contiguous cell sheet, thus preserving cell-to-cell junction proteins and native extracellular matrix (ECM) secreted by the cells [6]. ECM has been shown to play an important role in improving propagation of stem cells and stem

* Corresponding author. Present address: Department of Surgery, National Taiwan University Hospital, 7 Chung-Shan S. Rd., Taipei 100, Taiwan. Tel.: +886 2 23123456x65068; fax: +886 2 23934358.
E-mail addresses: nccheng@ntu.edu.tw, naichenc@gmail.com (N.-C. Cheng).
[1] These two authors contributed equally to this work.

0142-9612/$ – see front matter © 2014 Elsevier Ltd. All rights reserved.
http://dx.doi.org/10.1016/j.biomaterials.2014.01.015

cell differentiation [7,8]. Previous investigators have adapted different techniques for cell sheet formation, such as the development of a temperature-responsive culture dish that could be used to harvest cultured cells and their deposited ECM non-invasively as intact sheets [9]. However, the entire grafting process has been criticized to be relatively complicated, time-consuming, and requires special materials [10]. Alternative approaches of using ascorbic acid to create cell sheets have also been proposed [5,10,11]. Ascorbic acid is not only a common nutrient vital to human health, it also plays a key role in the biosynthesis of collagen and other ECM constituents [12]. By supplementing ascorbic acid in the culture medium, cell sheets derived from human MSCs of various tissue origin can be fabricated in 7–10 days [10].

Ascorbic acid has been used as a supplement for culture of various cell types. In addition to stimulating ECM production, it can also act as an antioxidant to suppress intracellular reactive oxygen species (ROS) levels and exert protective effects on cells [13,14]. Ascorbic acid can also stimulate cellular proliferation and DNA synthesis of MSCs during *in vitro* culture [15]. Moreover, ascorbic acid has been shown to enhance the generation of mouse and human induced pluripotent stem (iPS) cells [16], and it can further enhances the cardiac differentiation of embryonic stem cells or iPS cells [17,18]. For MSCs, a previous report also showed that ascorbic acid can inhibit differentiation and upregulate pluripotent marker expression of *Oct4* and *Sox2* [19]. Therefore, the addition of ascorbic acid during *in vitro* culture of stem cells is considered to be beneficial. However, the use of ascorbic acid is limited by its rapid oxidation [20]. L-ascorbic acid 2-phosphate (A2-P), a more stable oxidation-resistant derivative of ascorbic acid, has been adapted in several studies and stimulated the growth of various cells more effectively [15,21–23].

The application of ASC-based cell sheet technology has been successful in creating tissue-engineered adipose substitute, treatment of myocardium infarction and enhancing skin wound healing [5,24,25]. However, the regenerative mechanism of ASC sheets is not well understood, and the differentiation capabilities of ASC sheets have not been fully investigated [10,26]. In this study, we tested the hypothesis that ASCs in a cell sheet format can maintain a stable undifferentiated status without loss of multipotency. We aimed to develop a practical method of A2-P-mediated ASC sheet formation, and we further examined the stemness and differentiation capabilities of ASCs within the cell sheets. The information is useful in elucidating the importance of ECM within cell sheets in maintaining the regenerative capabilities of stem cells, so it should benefit the future application of cell sheet-based tissue engineering.

2. Materials and methods

2.1. Cell culture

Subcutaneous adipose tissue from abdomen was obtained from 5 female donors undergoing abdominoplasty procedures with an average age of 42 (range 30–57) and an average body mass index (BMI) of 24.8 (range 21.0–26.6). The study protocol was approved by the Internal Ethical Committee of National Taiwan University Hospital. The adipose tissue was placed in a physiological solution (0.9% NaCl), washed twice with phosphate-buffered saline (PBS; Omics Biotechnology, Taipei, Taiwan) and finely minced. The scraped adipose tissue was then placed in a digestion solution: 1 mg/ml collagenase type I (Gibco, Carlsbad, CA) dissolved in PBS, at 37 °C in agitation for 60 min. After digestion, the cell suspension was filtered through 40 μm cell strainers (BD Falcon, Franklin Lakes, NJ). The cells were cultured in expansion medium consisting of Dulbecco's modified Eagle's medium (DMEM)/F-12 (Hyclone, Logan, UT), 10% fetal bovine serum (FBS; Biological industries, Kibbutz Beit Haemek, Israel), 1% 1% antibiotic-antimycotic (Biological Industries), and 1 ng/ml basic fibroblast growth factor (bFGF; R&D systems, Minneapolis, MN). The cells were cultured at 37 °C in 5% CO_2, and the medium was changed every 2 days. When the cells have reached 90% confluence, the cells were lifted with 0.05% trypsin-EDTA (Biological Industries) and replated.

2.2. Cell sheet formation

Third passage ASCs were harvested or further experiments. To create cell sheets, 5×10^5 ASCs were cultured in a 100 mm culture dish for 7 days. The culture medium consisted of DMEM-HG (Gibco), 10% FBS, 1% antibiotic-antimycotic, and 250 μM A2-P (Sigma). The medium without A2-P was used in the control group. The culture medium was refreshed every 2–3 days. Cells with or without A2-P treatment were also subjected to analyses including reverse transcription-polymerase chain reaction (RT-PCR), immunofluorescence, and western blotting. U0126, an inhibitor of ERK1/2, was prepared in DMSO and used in ERK1/2 signaling inhibition assay. The concentration of U0126 used was 5 μM, which did not affect APCs proliferation in our pilot study. The ERK signaling in the long-term culture was checked by treating the cells with A2-P or U0126 for 3 days.

2.3. Flow cytometry analysis

After treatment with or without 250 μM A2-P for 7 days, ASCs were subjected to flow cytometry analysis to determine cell surface antigen expression. The cells were incubated with the following antibodies: human monoclonal antibodies against CD31 (BD pharmingen, San Jose, CA), CD34, CD73, CD90 (all from BioLegend, San Diego, CA), CD105 (eBioscience, San Diego, CA) and CD166 (BioLegend). The samples were analyzed using a flow cytometer (FACScan; Becton Dickinson, Franklin Lakes, NJ) which counts 10,000 cells per sample. Positive cells were determined as the proportion of the population with higher fluorescence than 95% of the isotype control.

2.4. Electron microscopy, histology and immunohistochemistry

For the electron microscopic study, cell samples were washed with PBS twice and fixed with 2.5% glutaraldehyde in PBS for 1 h. After thoroughly washing with PBS, the cells were dehydrated by gradual change of concentrated ethanol and then dried by lyophilization. The specimens were then sputter coated with platinum and examined using a scanning electron microscope (JSM-6700F, JOEL, Tokyo, Japan).

ASC sheets induced by A2-P treatment could be easily detached from tissue culture plates and fixed in 4% paraformaldehyde for paraffin-embedded histological analysis. Sections were cut perpendicular to the surface of the cell sheet into a thickness of 5 μm. Paraffin-embedded sections were rehydrated and stained with hematoxylin and eosin (H&E, Sigma) and Masson's trichrome stain (Sigma). Immunohistochemical analysis was performed using anti-collagen type I (Epitomics, Burlingame, CA), anti-fibronectin (Epitomics) and anti-laminin (Pierce Biotechnology, Rockford, IL). Bovine serum albumin (BSA, Santa Cruz, Santa Cruz, CA) was used on all sections before secondary antibody labeling, followed by subsequent linking to horseradish peroxidase and substrate/chromogen reaction using immunoperoxidase secondary detection kit (Millipore, Billerica, MA). Negative controls without utilizing primary antibodies were also prepared to rule out nonspecific labeling.

2.5. Cell proliferation assay and growth curve

The cell proliferation assay was performed by measuring double-strand DNA (dsDNA) content of the ASCs. Cells were seeded at a density of 5×10^3 cells per well in 24-well plates with or without 250 μM A2-P. On day 1, 4, 7, DNA content was measured fluorometrically using the Quant-iT Picogreen dsDNA Reagent and Kits (Invitrogen) according to the manufacturer's protocol (excitation wavelength, 485 nm; emission wavelength, 535 nm). Moreover, ASCs were seeded at a density of 2.5×10^5 cells per 100 mm culture dishes with or without 250 μM A2-P treatment. Every 7 days, cells were lifted, counted with Scepter™ 2.0 Cell Counter (Millipore), and replated. The process was repeated until cells reached senescence.

2.6. Differentiation of human ASCs

ASCs were pretreated with or without 250 μM A2-P for 7 days before induction of differentiation. Adipogenic differentiation was induced in DMEM-HG supplemented with 10% FBS, 1% antibiotic-antimycotic, 500 μM 3-isobutyl-1-methylxanthine (IBMX; Sigma, St. Louis, MO), 1 μM dexamethasone (Sigma), 10 μM insulin (Sigma) and 400 μM indomethacin (Sigma). After 9 days, the cells were fixed in 4% paraformaldehyde and stained with Oil Red O (Sigma) to observe lipid droplets. Then the dye was eluted by isopropanol and measured by a spectrometer (μQuant, BIOTEK, Seattle) at 510 nm. Osteogenic differentiation was induced by culturing ASCs in DMEM-HG supplemented with 10% FBS, 1% antibiotic-antimycotic, 10 nM dexamethasone, 50 μM A2-P, 10 nM 1α,25-Dihydroxyvitamin D_3 (Sigma), and 10 mM β-glycerophosphate (Sigma). After 9 days, ASCs were fixed in 4% paraformaldehyde and stained with Alizarin red S (Sigma) to observe mineralized matrix apposition. The bound Alizarin red S was extracted by 10% hexadecylpyridinium chloride monohydrate (Sigma), and the absorbance of dye was measured at 550 nm. Quantification of ASC adipogenic and osteogenic differentiation was estimated by normalizing the absorbance of the eluted dye to the dsDNA content within each well.

To induce neurogenic differentiation, the cells were cultured in DMEM-HG containing 1% FBS, 1% antibiotic-antimycotic and 100 ng/ml bFGF (R&D) for 7 days, followed by supplementation with 100 ng/ml bFGF and 10 μM forskolin for another 7 days [27]. At day 14, the expression of neurogenic differentiation markers, Nestin and GFAP, was analyzed by RT-PCR, western blot and immunofluorescence. Hepatogenic differentiation was induced in DMEM-HG medium with 1% antibiotic-antimycotic, 20 ng/ml epidermal growth factor (R&D) and 10 ng/ml bFGF for 48 h. In

the following days, 10% FBS, 20 ng/ml hepatocyte growth factor (R&D), 10 ng/ml bFGF, 4.9 mM nicotinamide were supplemented in the culture medium [28]. At day 16, the expression of hepatogenic markers, Albumin and CYP3A4, was analyzed by RT-PCR, western blot and immunofluorescence.

2.7. Intracellular ROS assay and total collagen assay

In some experiments, ASCs were treated with antioxidants N-acetyl-L-cysteine (NAC) or L-Glutathione reduced (GMEE). The cells were pretreated with 250 μM A2-P, 1 mM NAC or 16.2 μM GMEE for 1 day, followed by incubating in 25 μM H_2O_2 for 30 min. Generation of intracellular ROS was evaluated by total ROS detection kit (Enzo life sciences, Farmingdale, NY). The optical density value was measured using fluorescence microplate reader (Tecan, San Jose, CA) at excitation and emission wavelengths of 550 and 610 nm, respectively.

Moreover, in certain A2-P-supplemented culture condition, 300 μM L-azetidine-2-carboxylic acid (AzC, Sigma) 300 μM or cis-4-hydroxy-D-proline (CIS, Sigma) 300 μM was added as collagen synthesis inhibitors. After 7 days of culture, collagen content was assessed by Sircol collagen assay (Biocolor, Newtownabbey, UK). Briefly, cells in each well were detached by HyQtase (Hyclone) treatment and discarded, and the remaining ECM was digested with 5 mg/ml pepsin (Roche, Indianapolis, IN) overnight. Then 0.5 ml Sircol dye reagent was added into each well and agitated to form collagen-dye complex, followed by centrifugation and dye release by alkali treatment. The absorbance of the released dye was measured by a spectrometer (Infinite F200, Tecan) at 570 nm.

2.8. RNA isolation and real-time RT-PCR

Total RNA was isolated using RNeasy® Mini Kit (Qiagen, Valencia, CA) according to the manufacturer's protocol. RNA concentration was determined by optical density at 260 nm (OD_{260}) using a spectrophotometer (Nanodrop ND-1000, Wilmington, DE). Once RNA was isolated, complementary DNA (cDNA) was synthesized from RNA using High-Capacity cDNA Reverse Transcription Kits (Applied Biosystems, Foster city, CA). The sequences of the gene-specific primers are shown in Table 1. Briefly, quantitative RT-PCR was performed using FastStart universal SYBR Green master (Roche) and CFX Connect™ Real-Time PCR Detection System (Bio-Rad, Hercules, CA). The expression level was analyzed and normalized to glyceraldehyde 3-phosphate dehydrogenase (GAPDH) for each cDNA sample. Relative quantity (RQ) of gene expression was calculated with comparative C_T method.

2.9. Western blot analysis

The protein expression of various experiments was determined by western blot analysis. The cells were suspended in cell lysis buffer (Fermentas, Vilnius, Lithuania) and sonicated. After centrifugation, the protein content was determined in the supernatants by a BCA protein quantification kit (Pierce Biotechnology). Sixty μg proteins were added to Laemmli sample buffer and boiled for 10 min. Proteins were separated by sodium dodecyl sulfate-polyacrylamide gel electrophoresis (SDS-PAGE) and blotted onto polyvinylidene difluoride membranes. Western blot was performed using anti-p21 (Cell Signaling, Danvers, MA), anti-laminin (Pierce Biotechnology), anti-fibronectin, anti-ERK1/2, anti-phospho-ERK1/2 (all from Epitomics), anti-Oct4, anti-Sox2, anti-Nanog (all from Genetex, Irvine, CA), anti-Nestin, anti-GFAP, anti-CYP3A4 and anti-human serum albumin (all from Abcam, Cambridge, MA), and anti-GAPDH (Genetex). The membranes were incubated with the primary antibodies overnight at 4 °C. After extensive washing, the membranes were further incubated with horseradish peroxidase-conjugated secondary antibodies for 1 h. The blots were then developed using an enhanced chemiluminescence detection system (Millipore).

Table 1
Primer sequences used in quantitative RT-PCR.

Target gene		Primer sequences
GAPDH	Forward	5′-CAAAGGCTGAGAACGGGAAGC-3′
	Reverse	5′-AGGGGGCAGAGATGATGACC-3′
Nanog	Forward	5′-CCTGTGATTTGTGGGCCTG-3′
	Reverse	5′-GACAGTCTCCGTGTGAGGCAT-3′
Oct-4	Forward	5′-GCAGCGACTATGCACAACGA-3′
	Reverse	5′-CCAGAGTGGTGACGGAGACA-3′
Sox-2	Forward	5′-CATCACCCACAGCAAATGACA-3′
	Reverse	5′-GCTCCTACCGTACCACTAGAACTT-3′
Nestin	Forward	5′-GGCAGCGTTGGAACAGAGGT-3′
	Reverse	5′-CATCTTGAGGTGCGCCAGCT-3′
GFAP	Forward	5′-GAGGCGGCCAGTTATCAGGA-3′
	Reverse	5′-GTTCTCCTCGCCCTCTAGCA-3′
Albumin	Forward	5′-TGT TGCATGAGAAAACGCCA-3′
	Reverse	5′-GTCGCCTGTTCACCAAGGA-3′
CYP3A4	Forward	5′-TTGCCCATTGTTTAGAAAGAAT-3′
	Reverse	5′-CCATGCCTAGCTAATTTGTG-3′
Fibronectin	Forward	5′-CTGGCCCGAAAATACATTGTAAA-3′
	Reverse	5′-CCAVAGTCGGGTCAGGAG-3′
Laminin	Forward	5′-CAGGACCCATTACCCTTTTG-3′
	Reverse	5′-GCCCTGCTTGGTTTCTTTATT-3′
COL1A1	Forward	5′-CCCTCAAGGTTTCCAAGGAC-3′
	Reverse	5′-ACCAGGTTCACCCTTCACAC-3′

2.10. In vivo wound healing model

At least five female nude mice (20–25 g body weight; National Laboratory Animal Center, Taipei, Taiwan) were used per condition in accordance with National Taiwan University animal care guidelines. On the day of surgery, two 9-mm round full-thickness cutaneous wounds were created on each side of the dorsal midline. Immediately after wounding, mitomycin C solution (1 mg/mL) was applied for 10 min to create a healing-impaired wound [29]. Then the wounds were circumscribed by donut-shaped silicone splints held in place using 6-0 nylon sutures to prevent wound contraction. A piece of ASC sheet or dissociated ASCs of comparable cell number (7.5×10^5 cells) in 100-μL PBS was applied to one of the dorsal wounds in each mouse. The contralateral wound was injected with 100-μL PBS as a control. The wounds were covered with a transparent, semi-occlusive adhesive dressing (Tegaderm, 3M, St. Paul, MN). Digital photographing of the wounds was taken regularly and the wound size was estimated using planimetric methods (Image J).

2.11. Immunofluorescence

The cultured cells were fixed in 4% paraformaldehyde, permeabilized in 0.1% Triton X-100 for 10 min at room temperature, immersed in 0.1% TritonX-100 for 10 min at room temperature, followed by washing 3 times with PBS. Then the following primary antibodies were incubated overnight at 4 °C: anti-Oct4, anti-Nanog, anti-Sox2 (all from Genetex), anti-Nestin, anti-GFAP, anti-CYP3A4 and anti-human serum albumin (all from Abcam). After incubation with primary antibodies, cells were washed with PBS and then incubated with fluorescence-conjugated secondary anti-rabbit IgG (Jackson Immounoresearch, West Grove, PA) for 1 h at room temperature. After nuclear staining with 4′,6-diamidino-2-phenylindole (DAPI, Santa Cruz), the cells were analyzed by a fluorescent microscope (Leica DMI 6000).

For immunofluorescence staining of the wound sections, the entire cutaneous wounds were harvested on postoperative day 14, including surrounding skin area of 0.5 cm. Tissue specimens were snap frozen in liquid nitrogen for frozen sections. Sections were made perpendicular to the anterior–posterior axis and perpendicular to the surface of the wound. Frozen sections were fixed with acetone and stained using anti-human nuclear antigen (HNA, Millipore) to detect transplanted human cells. Sections were also subjected to immunofluorescent staining with anti-CD31 for vascular structures in the wound, or they were stained with pancytokeratin (Abcam) for detecting epidermal cells. DAPI counterstaining was performed and double-immunolabeled cells (CD31+/HNA+ or pancytokeratin+/HNA+) were quantified in 10 different images per slide from 5 different samples.

2.12. Statistical analysis

All measurements are presented as means ± standard deviation. Statistical significance was evaluated using an independent-samples Student's *t*-test or ANOVA followed by Scheffé's post-hoc test. All statistical analyses were performed using STATA software (Stata Inc, Collage Station, TX). Statistically significant values were defined as $p < 0.05$.

3. Results

3.1. Characterization of ASCs

Human ASCs cultured with or without 250 μM A2-P for 7 days were dissociated for flow cytometry. The surface epitopes of A2-P-treated ASCs were similar to those of ASCs without A2-P treatment. These ASCs were negative for hematopoietic markers CD31 and CD34, and were positive for MSC-related markers CD73, CD90, CD105, and CD166 (Fig. 1A). A2-P-treated ASCs maintained their adipogenic and osteogenic differentiation capabilities after application of appropriate induction media, as demonstrated by histology staining specific for oil and calcium, respectively. Moreover, quantification of the bound oil red O or Alizarin S dyes after adipogenic or osteogenic induction showed no significant difference in ASCs with or without previous A2-P treatment (Fig. 1B).

Cell number estimated by dsDNA assay demonstrated ASC proliferation in both culture conditions with or without A2-P. However, on day 4 and 7 of culture, the dsDNA content of A2-P-

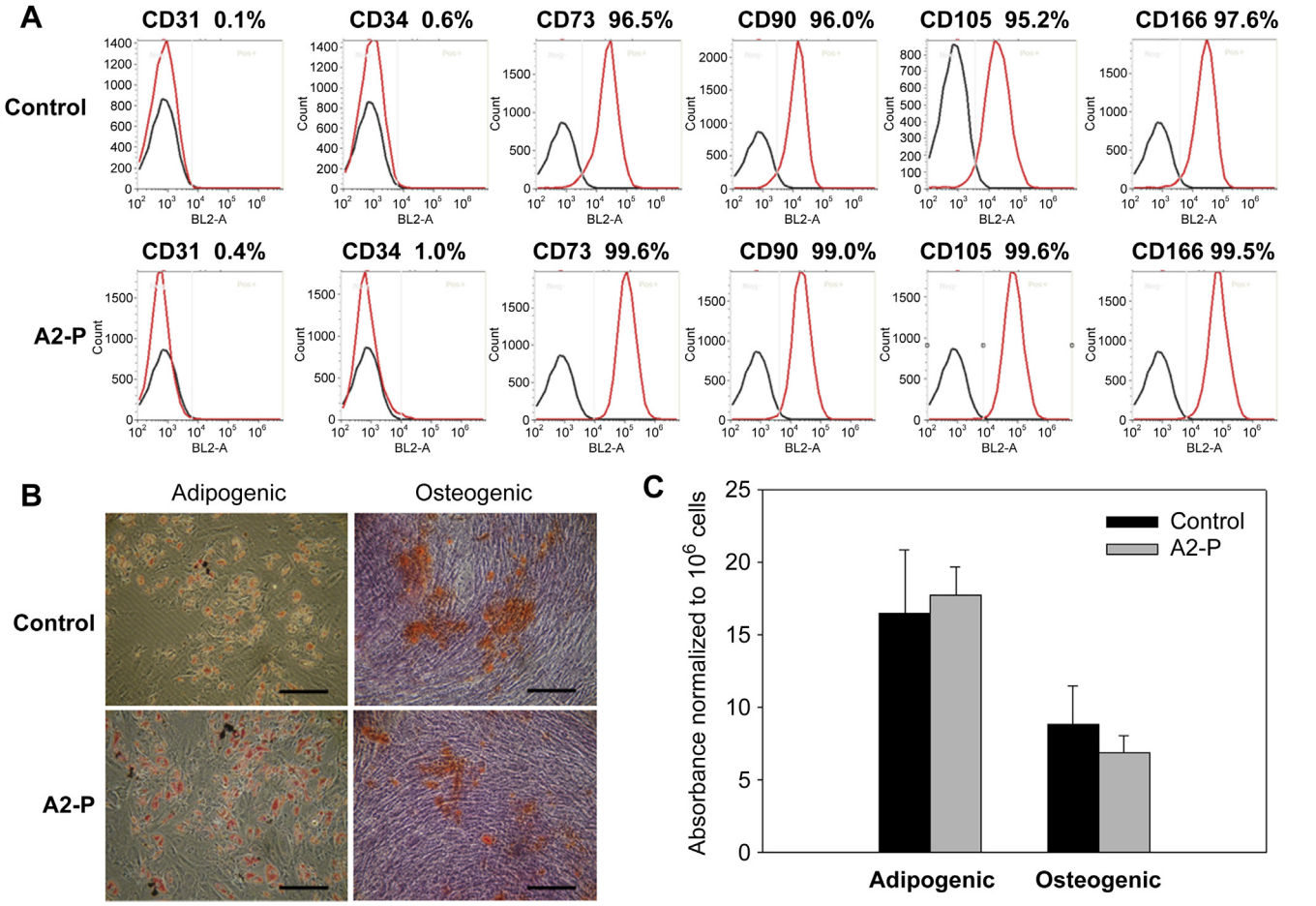

Fig. 1. Phenotypic characterization of ASCs cultured with or without A2-P. (A) The ASCs were plated in monolayer cultures with or without A2-P for 7 days. The expression level of ASC surface antigens was determined by flow cytometry and shown as the proportion of positively stained cells relative to an isotype control. (B) ASCs cultured with or without A2-P for 7 days were further cultured in adipogenic or osteogenic induction medium for 9 days. Cell cultures were stained with Oil Red O for detection of adipogenesis and Alizarin Red for detection of osteogenesis. Scale bar = 100 μm. (C) Dye absorption measurements for Oil Red O and Alizarin Red in ASCs at day 9 of adipogenic and osteogenic induction culture. No significant difference between the cells with or without previous exposure to A2-P was noted.

treated ASCs was significantly higher than the control group (51.2 ± 3.4 vs. 41.0 ± 5.0 μg per well at day 4, $p < 0.05$; 82.3 ± 2.1 vs. 66.3 ± 1.4 μg per well at day 7, $p < 0.01$; Fig. 2A). Moreover, A2-P-treated ASCs expanded more rapidly through passages compared to ASCs without A2-P treatment, but A2-P-treated ASCs appeared to reach senescence earlier than the control cells (Fig. 2B). The expression of p21 protein, a senescence marker, also appeared to increase under A2-P treatment throughout the passages (Fig. 2C).

3.2. A2-P-induced cell sheet formation

Under electron microscopy, ASCs on the surface of the A2-P-induced cell sheet appeared to intermingle with each other closely, and it was difficult to distinguish the cellular boundary. Meanwhile, ASCs without A2-P treatment exhibited spindle-shape morphology with clearly-delineated cell margins (Fig. 3A). Cell sheets were also peeled off from the tissue culture plates and subjected to histological and immunohistochemical examination of their cross sections. H&E staining showed 2 or 3 layers of ASCs within the cell sheet with abundant ECM formation within the interstitial voids of the cells. Masson's trichrome staining also showed abundant collagen deposition within the ASC sheet (Fig. 3B). Moreover, immunohistochemistry revealed a robust meshwork of collagen type I, fibronectin and laminin inherent with its endogenous ECM in ASC sheets (Fig. 3C).

RT-PCR analysis revealed 3.7 ± 1.2 fold upregulated *COL1A1*, 4.9 ± 1.9 fold upregulated *Fibronectin* and 9.9 ± 1.7 fold upregulated *Laminin-α1* genes in ASC sheets, and all these genes exhibited significantly more transcripts than the control ASCs (Supplementary Fig. 1). In A2-P-treated ASCs, significant higher collagen content was determined by Sircol collagen assay (Fig. 6B), and significantly more fibronectin and laminin production was also found by western blot analysis (Fig. 3D). We further examined the activity of ERK signaling because collagen synthesis is associated with the regulation ERK1/2 pathway [30,31]. The western blot results showed that A2-P significantly attenuated ERK signaling in ASCs. By applying an inhibitor of ERK1/2 pathway, U0126, a similar pattern of enhanced fibronectin and laminin production was observed, though the increment was not statistically significant (Fig. 3E). Therefore, A2-P may stimulate ECM production of ASCs partially through attenuating ERK signaling pathway.

3.3. The expression of stemness markers in ASC sheets

The relative mRNA expression of pluripotency-associated transcription factors *Nanog*, *Oct4* and *Sox2* were analyzed by RT-PCR. At day 3 of culture, ASCs with or without A2-P treatment exhibited no

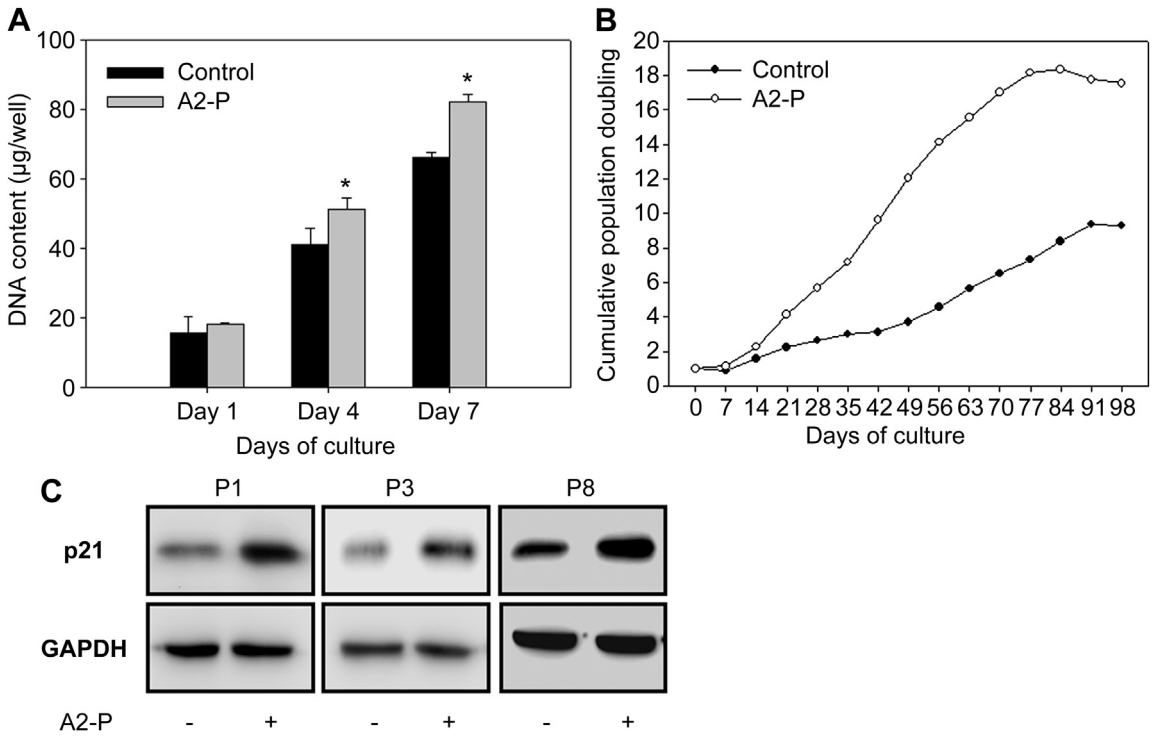

Fig. 2. A2-P-treated ASCs exhibited higher growth rate. (A) Quantification of dsDNA to estimate cell proliferation; $^{*}p < 0.05$, compared to the control group at the same time point ($n = 3$). (B) Cumulative population doubling curve of ASCs treated with or without A2-P. Cells were plated at low density and passaged every 7 days. (C) Western blot analysis for senescence marker p21 showed more p21 expression in A2-P-treated ASCs at different passages.

difference regarding the expression of Nanog, Oct4 and Sox2. However, ASCs exhibited significant upregulation of *Nanog*, *Oct4* and *Sox2* genes after 7 days of A2-P treatment, with 3.8 ± 0.1-fold, 2.2 ± 0.2-fold and 3.8 ± 0.1-fold increase from the control ASCs respectively (Fig. 4A). Western blot analysis also showed more protein expression of Sox2, Oct4 and Nanog in day 7 ASC sheets comparing to control ASCs (Fig. 4B). Analyses of immunofluorescence images further confirmed the enhanced expression of these stemness markers in ASC sheets relative to the control group (Fig. 4C).

3.4. Enhanced ASC transdifferentiation in cell sheets

While A2-P-induced ASC sheet formation maintained the differentiation capabilities along the mesenchymal lineages of ASC, we observed enhanced transdifferentiation capabilities of ASC sheets. After hepatogenic induction medium was applied, RT-PCR revealed significantly more gene transcripts of *Albumin* and *CYP3A4* in ASC sheets comparing to control ASCs, with estimated 13.5 ± 2.6 vs. 8.5 ± 1.0-fold upregulation for *Albumin* ($p < 0.05$) and 5.1 ± 0.5 vs. 2.8 ± 0.1-fold upregulation for *CYP3A4* ($p < 0.01$). Western blot and immunofluorescence analyses of these two important hepatogenic differentiation markers further confirmed the enhanced protein expression of Albumin and CYP3A4 in ASC sheets relative to control ASCs (Fig. 5A).

After application of neurogenic induction medium to ASC sheets and monolayer ASCs, RT-PCR also revealed significantly more gene transcripts of *Nestin* and *GFAP* in ASC sheets. Relative to control ASCs, ASC sheets exhibited 4.4 ± 0.9 vs. 2.2 ± 0.1-fold upregulation for *Nestin* ($p < 0.05$) and 2.3 ± 0.3 vs. 1.4 ± 0.3-fold upregulation for *GFAP* ($p < 0.05$). Protein expression of these two important neurogenic differentiation markers, Nestin and GFAP, as demonstrated by western blot and immunofluorescence, also showed enhanced expression in ASC sheets relative to ASCs without previous A2-P treatment (Fig. 5B).

3.5. Influence of collagen synthesis inhibitors and antioxidants on stemness

The favorable effects of ascorbic acid on cells can be attributed to its antioxidative or collagen synthesis properties [16–18]. Therefore, we investigated the mechanism of enhanced stemness in ASC sheets by using two antioxidants (NAC and GMEE) and two types of collagen synthesis inhibitors (AzC and CIS) [16]. NAC 1 mM or GMEE 16.2 μM in the ASC culture medium significantly decreased the intracellular ROS level to a level comparable to 250 μM A2-P (Fig. 6A). To examine whether AzC or CIS actually inhibits collagen synthesis in A2-P-treated ASCs, collagen content was quantified by Sircol collagen assay. A2-P treatment significantly increased collagen production of ASCs, and AzC treatment significantly inhibited A2-P-induced collagen synthesis to a level comparable with the control group at day 7 of culture. Meanwhile, CIS only partially inhibited collagen synthesis induced by A2-P (Fig. 6B).

Unlike that A2-P increased the mRNA expression of stemness markers *Nanog*, *Oct4* and *Sox2* in ASCs, RT-PCR analysis revealed no significant upregulation of these markers in ASCs with NAC or GMEE treatment. Moreover, when a collagen synthesis inhibitor (AzC or CIS) was supplemented with A2-P treatment, the enhanced mRNA expression of *Nanog*, *Oct4* and *Sox2* was also inhibited, except that Nanog still exhibited a significant 2.8 ± 0.6-fold upregulation in A2-P + CIS treatment group (Fig. 6C). Similar to the mRNA expression pattern, western blot showed that A2-P-induced ASC sheet formation increased protein expression of the stemness markers, and this increase was inhibited by AzC or CIS treatment.

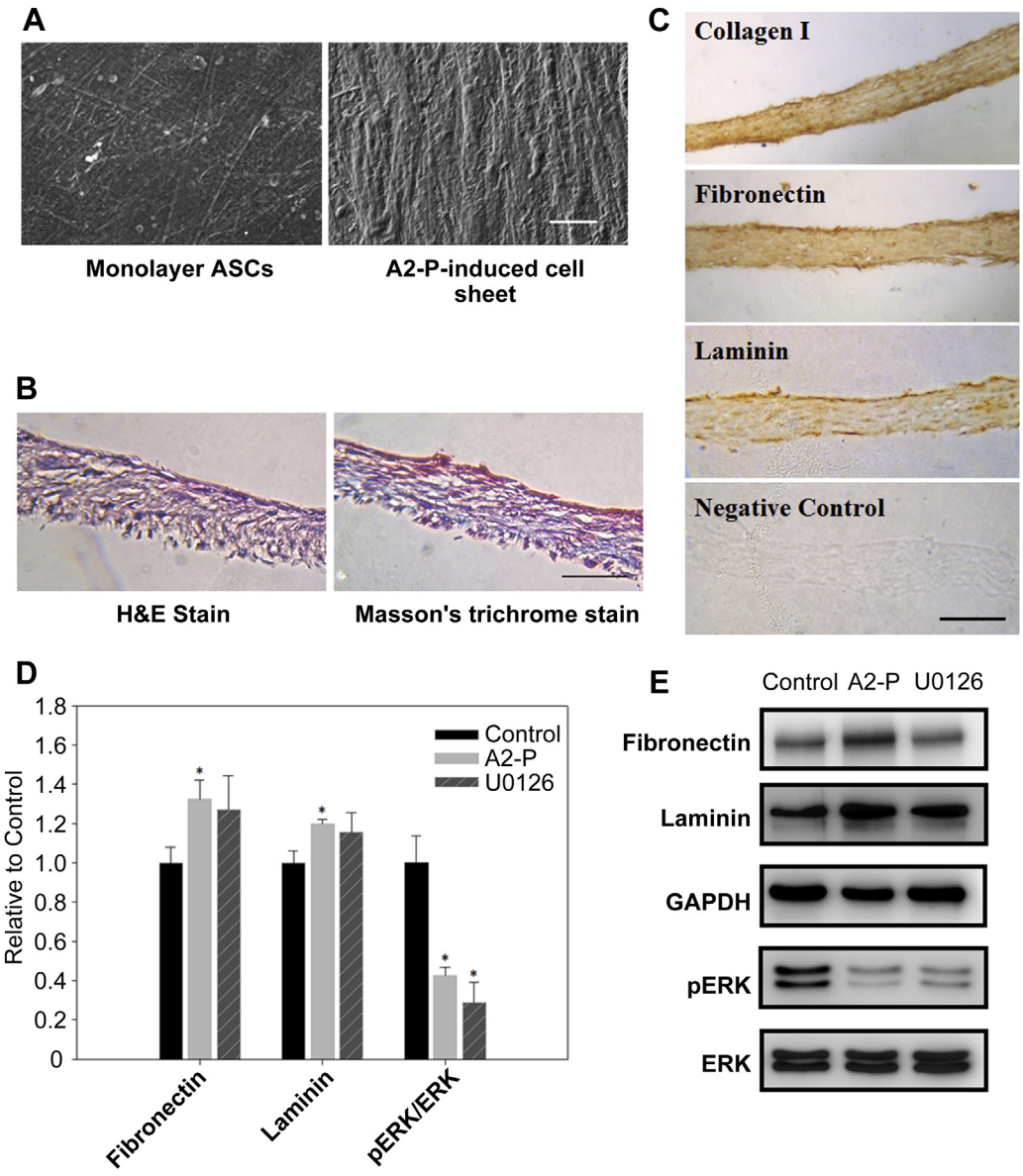

Fig. 3. Cell sheet formation of ASCs after 7 days of culture with A2-P. (A) Scanning electron microscopic image of ASCs with A2-P treatment revealed cell sheet formation with an indistinguishable cell–cell junction. Scale bar: 20 μm. (B) H&E and Masson's trichrome histological staining of the cross section of A2-P-induced ASC sheets. Scale bar: 20 μm; (C) Immunohistochemistry revealed abundant ECM molecules (collagen type 1, fibronectin and laminin) in ASC sheets. Scale bar: 50 μm. (D) Equal amounts of protein from control, A2-P and U0126 -treated cells were subjected to electrophoresis and western blotting. Densitometric measures of the band intensity are expressed as the protein expression ratios relative to control ASCs. A2-P-treated ASCs exhibited significantly enhanced fibronectin and laminin expression with decreased p-ERK/ERK signal, which indicates the level of ERK1/2 phosphorylation. U0126 also could inhibit ERK signaling, but the increase of fibronectin and laminin expression was not statistically significant. Data presented as mean relative density ±SD; $^{*}p < 0.05$, compared to the control group ($n = 3$). (E) Representative western blot images are shown.

Western blot analysis for NAC or GMEE-treated ASCs also revealed no enhanced Nanog, Oct4 and Sox2 expression (Fig. 6D).

3.6. Cell sheet for wound healing in vivo

To assess the regenerative capability of ASC sheets *in vivo*, we utilized a murine model of impaired cutaneous wound healing with topical mitomycin application [29]. When treated with ASC sheets, significantly smaller wound area was observed on post-wounding day 11, compared to those treated with PBS (Fig. 7A). To further investigate ASC differentiation in the wound, immunofluorescent staining of HNA and cell lineage-specific marker CD31/pan-cytokeratin was performed in wound sections harvested at day 14 after wound creation. Wounds that received ASC sheets exhibited a significantly higher number of CD31+/HNA+ cells compared with the dissociated ASC group (8.1 ± 3.9 vs. 1.4 ± 1.1 cells per high power field (hpf), $p < 0.05$). Similarly, significantly more pan-cytokeratin+/HNA+ cells were found in the cell sheet group relative to the dissociated ASC group (7.1 ± 2.3 vs. 1.7 ± 1.3 cells per hpf, $p < 0.05$). Co-localization of HNA and CD31 immunofluorescence indicated the differentiation of transplanted ASCs toward endothelial lineage, while HNA-positive cells co-localizing with pan-cytokeratin immunofluorescence indicated ASCs' contribution to the regeneration of epidermal structures (Fig. 7B). HNA immunofluorescence was not observed in wounds treated with PBS alone.

4. Discussion

Cell sheet engineering to create functional tissue sheets exhibits great potentials to treat a wide range of diseases from corneal

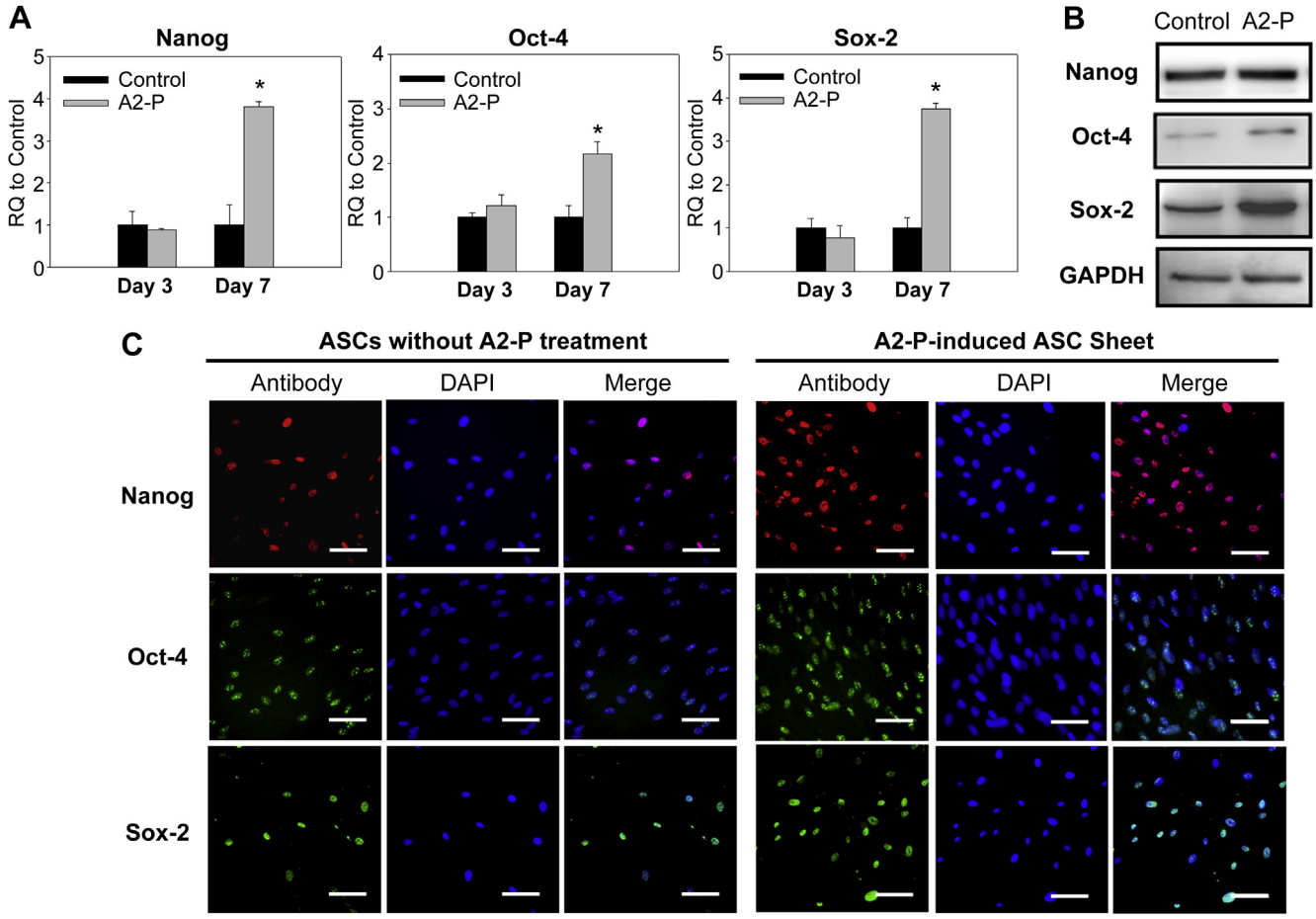

Fig. 4. Expression of stemness markers in ASCs treated with or without A2-P. (A) RT-PCR measurements for embryonic stem cell marker genes (*Oct-4*, *Sox-2* and *Nanog*). Values are mean relative quantity (RQ) ± SD compared with day 0 ASC sample; $^{*}p < 0.05$, compared to the control group ($n = 3$). (b) Western blot analysis of the expression of embryonic stem cell markers Oct-4, Sox-2 and Nanog. (c) Representative immunofluorescence of Oct-4, Sox-2 and Nanog in ASCs after 7 days of culture with or without A2-P. All nuclei were stained with DAPI (blue). Scale bar: 50 μm. (For interpretation of the references to color in this figure legend, the reader is referred to the web version of this article.)

dysfunction to esophageal cancer, tracheal resection, and cardiac failure [32]. Cell sheets composed of ASCs have also been shown to substantially enhance tissue regeneration and wound healing [5]. In this study, we employed A2-P, a stable form of ascorbic acid, to effectively fabricate transferable ASC sheet in a short time. Histology and immunohistochemistry showed abundant deposition of ECM molecules, including collagen, fibronectin and laminin, within the cell sheets after 7 days of ASC culture. Moreover, the stemness and differentiation capabilities of ASCs were well maintained in the cell sheet format. As a previous study revealed that A2-P enhanced DNA synthesis of bone marrow-derived MSCs during *in vitro* culture [15], A2-P-treated ASCs exhibited higher proliferative activity compared to control ASCs. Together with the A2-P-induced ECM deposition, expansion-promoting effect of A2-P enabled rapid fabrication of ASC sheets. However, we also found that these cells reached senescence at a time point earlier than cells without A2-P treatment during long-term cell culture. Moreover, at different passages during *in vitro* culture, A2-P-treated ASCs appeared to express a higher quantity of the senescence marker p21. Since cell–cell contact in the hyperconfluent culture of MSCs accelerates replicative senescence [33], it is possible that A2-P-induced cell sheet formation also results in premature exhaustion of the self-renewal potential of ASCs. The finding was in line with a recent study showing that adult stem cells have evolved a unique, p21-activation response to DNA damage that leads to their immediate expansion and limits their long-term survival [34]. Although the fabrication of ASC sheets may be associated with an accelerated impairment of their regenerative potential after prolonged *in vitro* culture, it should not be a hurdle for ASC-based cell sheet engineering since only the early passages of ASCs are suggested for clinical use [35].

The maintenance of pluripotency in embryonic stem cells has been attributed to several important transcription factors, including Oct4, Sox2 and Nanog [36]. The presence of these pluripotent markers has also been identified in adult stem cells, including ASCs, and they exert great influence on their self-renewal and differentiation capabilities [37]. However, the expression of the pluripotent genes declined with *in vitro* passaging of ASCs [38], which may represent a hindrance for the development of ASC-based regenerative therapy. In this study, the expression of stemness markers Oct4, Sox2 and Nanog was significantly enhanced relative to the control ASCs after 7 days of A2-P-supplemented cell culture, and we further investigated the possible mechanisms of A2-P-enhanced stemness in ASCs. Ascorbic acid can exert beneficial effects on cells by suppressing intracellular ROS production [13,14], but we showed here that alternative antioxidants (GMEE and NAC) failed to mimic the stemness-promoting role of A2-P on ASCs. Then we investigated the association of A2-P-induced collagen deposition with the enhanced stemness of ASCs. By supplementing the collagen synthesis inhibitors AzC and CIS in ASC culture, the A2-P-

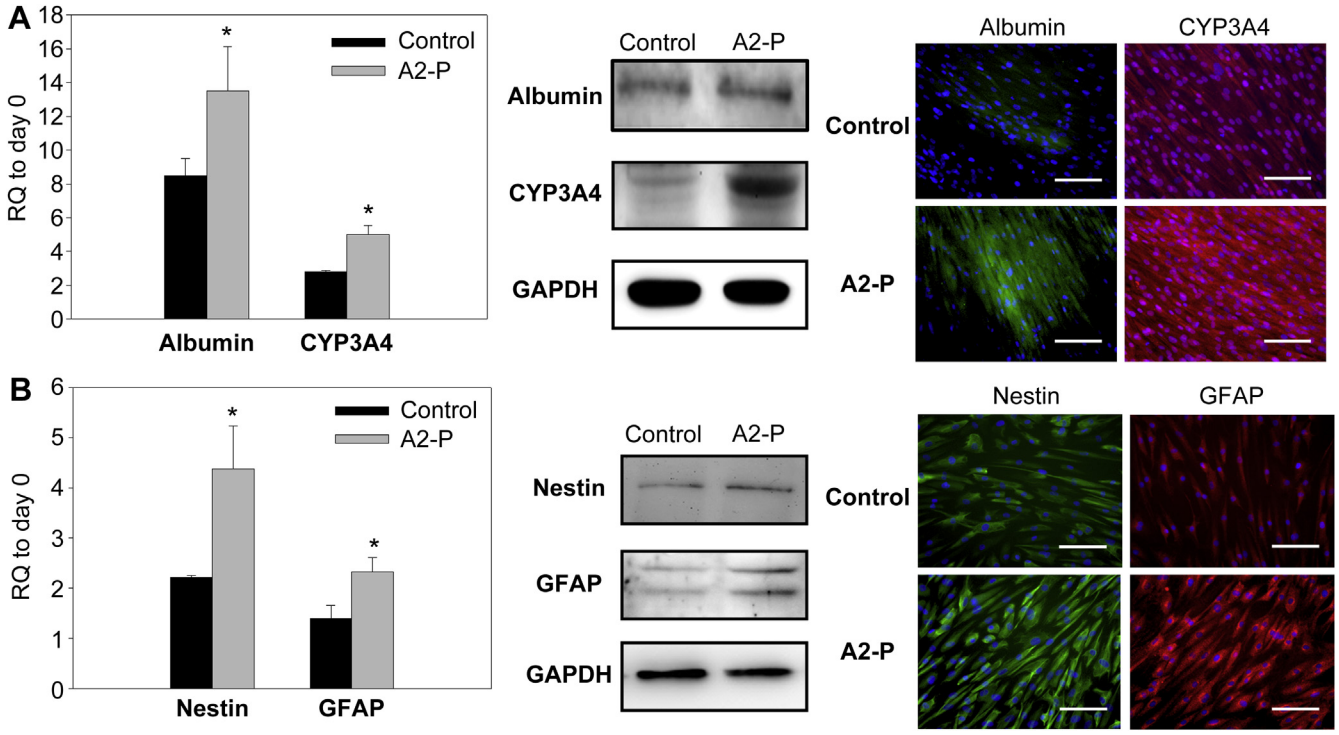

Fig. 5. Expression of (A) hepatogenic or (B) neurogenic transdifferentiation markers in ASC sheets and monolayer ASCs under respective induction medium for 14 days. RT-PCR measurements of hepatogenic markers (*Albumin* and *CYP3A4*) or neurogenic markers (*Nestin* and *GFAP*). RT-PCR values are mean RQ ± SD; $^{*}p < 0.05$, compared to the control group ($n = 3$). Western blot and Immunofluorescence images of Albumin and CYP3A4 for hepatogenic induction and Nestin and GFAP for neurogenic induction. Scale bar: 100 μm.

associated enhanced expression of stemness markers could be eliminated. Moreover, significant upregulation of stemness markers (*Oct4*, *Sox2* and *Nanog*) was observed only at day 7 of A2-P-supplemented ASC culture, but not day 3, at which time point cell sheet formation was not complete. Therefore, we clearly demonstrated that A2-P-induced collagen synthesis was required for stemness enhancement in ASCs. By applying U0126, an inhibitor of ERK1/2 pathway, we further showed that A2-P-induced deposition of ECM molecules, such as fibronectin and laminin, may be associated with the inactivation of ERK1/2 pathway in ASCs.

The importance of A2-P-associated ECM deposition in maintaining the stemness of ASCs is not surprising. For most types of cells, the cell behaviors, like attachment and proliferation, depend largely on their surrounding ECM, which are inherent with the resident cells [39]. By allowing interactions of cells with the surrounding ECM to adapt to their native morphology, significant differences between the cellular phenotype and biological response of cells cultured in monolayer and three-dimensional environment have been observed. Increasing data have also shown the importance of the ECM on stem cell fate determination through physical cell support and control of cell shape and geometry as a function of surface topography, substrate stiffness, and biochemical signaling [39]. For example, a porous cartilage-derived matrix from porcine articular cartilage that can support *in vitro* chondrogenic differentiation of ASCs [8,40]. Recently, it has been shown that ECM derived from MSCs can promote proliferation of MSCs and maintains their high responsiveness to the osteogenic and adipogenic inductive medium during *in vitro* culture [41,42]. Therefore, the use of continuous cell sheets, with the preservation of cellular junctions, endogenous ECM, and cellular microenvironments mimicking the inherent mechanical, chemical, and biological properties of cellular niche, should be beneficial for ASC-based tissue engineering.

A previous study showed that adipogenic and osteogenic (mesoderm) differentiation capacities of ASCs were maintained after cell sheet formation [26], which was in line with the results of this study. However, we further demonstrated that ASCs within cell sheets exhibited significantly enhanced neurogenic (ectoderm) and hepatogenic (endoderm) transdifferentiation capabilities comparing to control ASCs when cultured in appropriate induction medium. Human ASCs can be reprogrammed to iPS cells with substantially higher efficiencies than those reported for human dermal fibroblasts [43], which suggested that ASCs remain in a relatively immature state that is prone to reprogramming to ground state pluripotency. Previously we also reported that ASCs in spheroid culture can be activated to express pluripotent markers with enhanced differentiation capabilities [37,44]. In this study, given the enhanced stemness marker expression of ASCs within cell sheets, it is possible that they were reprogrammed to a more undifferentiated state with enhanced plasticity, thereby increasing their capabilities to transdifferentiate into cells of non-mesenchymal lineages.

In a mouse model of impaired wound healing, ASC sheet-treated wounds experienced a significant increase in the rate of wound closure compared to wounds treated with an equal number of ASCs delivered in suspension. Previous studies have demonstrated improvements in wound healing by injecting dissociated MSCs into wounds [45–47], but we appreciated a significant enhancement in healing only in the wounds treated by ASC sheets. These prior studies used 1.5 to 3 times as many MSCs as our injection studies, and a high level of cell death was observed within a few days after cell transplantation into ischemic tissue [45,47]. Therefore, ASC sheets can significantly enhance wound healing at a lower therapeutic dose relative to previously reported for dissociated ASCs. Moreover, application of ASC sheets onto cutaneous wounds avoids

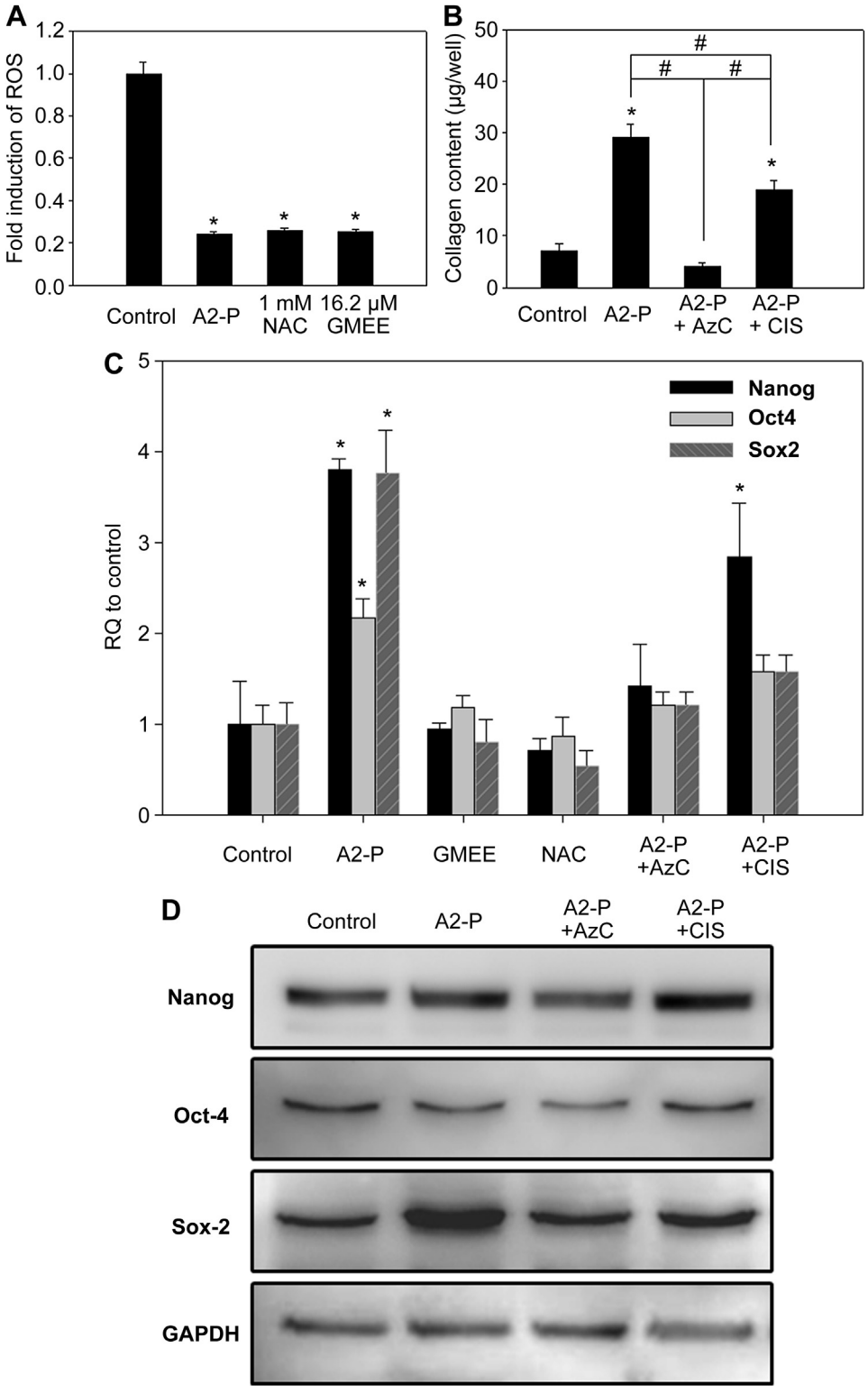

Fig. 6. Expression of stemness markers in A2-P-treated ASCs is associated with collagen synthesis. (A) ROS production of ASCs treated with A2-P and two other anti-oxidatives (GMEE and NAC). *$p < 0.05$ from the control group. (B) Collagen synthesis of ASCs was promoted by A2-P, which could be partially inhibited by AzC or CIS. *$p < 0.05$ from the control group; #$p < 0.05$ between the indicated groups. (C) RT-PCR measurements for pluripotent marker genes (*Nanog*, *Sox-2* and *Oct-4*) in ASCs after treatment with A2-P, GMEE, NAC, A2-P + AzC and A2-P + CIS. *$p < 0.05$ from the same gene in the control group. (D) Western blot analysis of the expression of pluripotent markers under different treatment conditions.

further tissue damage associated with transplantation of dissociated ASCs by needle injection. Immunofluorescent staining of the wound sections further revealed more co-localization of ASC with CD-31 and pancytokeratin immunofluorescence in the wounds treated with ASC sheets, suggesting enhanced plasticity of ASC sheets to contribute to endothelial and epithelial cell populations within healing cutaneous wounds. Thus, both our *in vitro* and *in vivo* data demonstrated higher transdifferentiation capabilities of

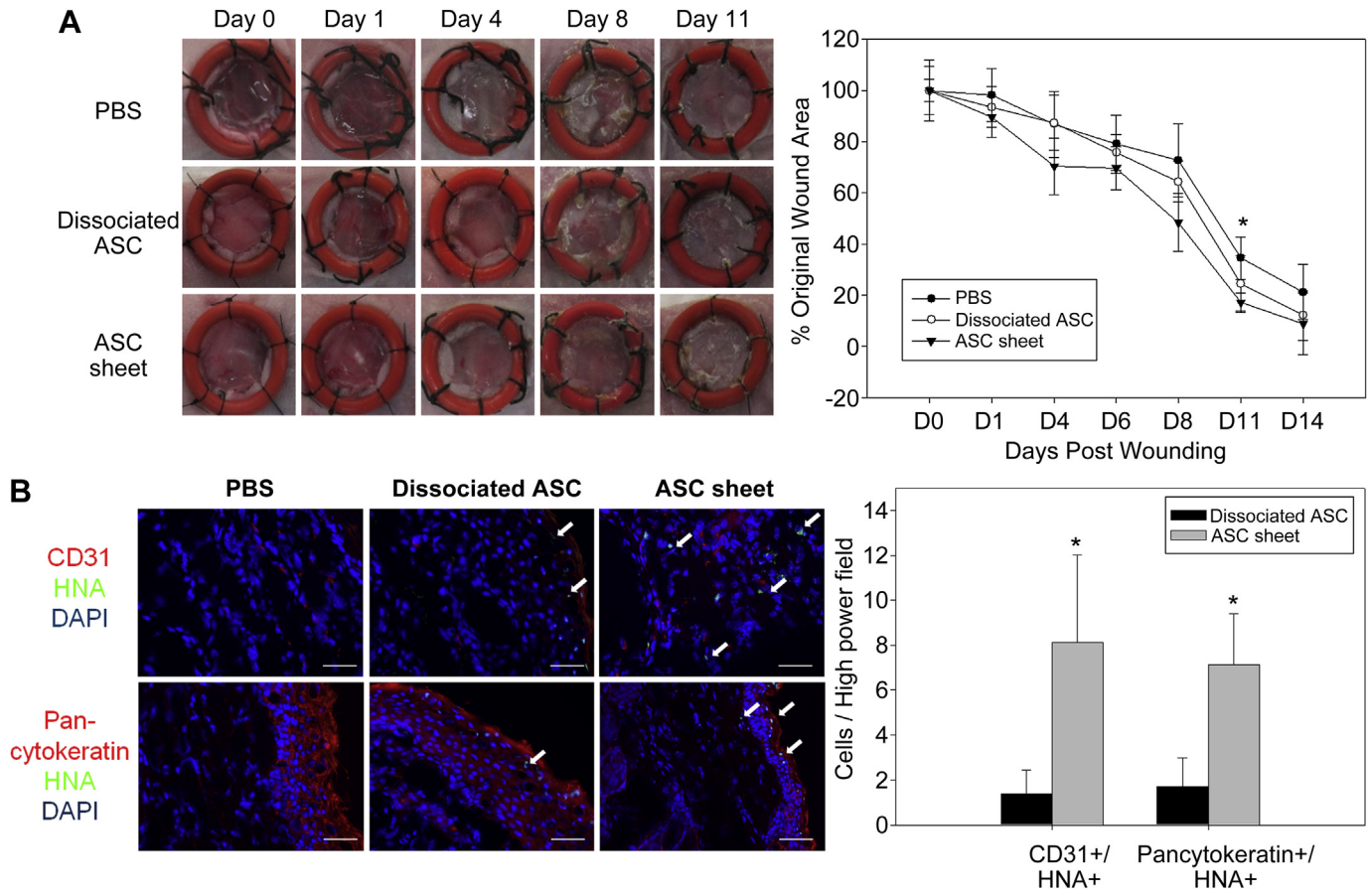

Fig. 7. Delivery of ASC sheet enhanced cutaneous wound closure in a mouse model. (A) Gross pictures and wound closure curves demonstrated accelerated healing in ASC sheet-treated wounds. $^{*}p < 0.05$ for the ASC sheet group from the PBS group. (B) Double immunofluorescent staining of HNA and an endothelial marker CD31 or an epidermal marker pancytokeratin in the day 14 wound sections. White arrows indicate co-localization of the HNA and CD31/pancytokeratin immunofluorescence, indicating human ASCs incorporated into vasculature or epidermal structure. The ratio of CD31+/HNA+ or pancytokeratin+/HNA+ cells among DAPI-stained cells was significantly higher in wound sections that received ASC sheet. Number of double immunofluorescence-positive cells was calculated from 10 randomly selected high power fields per sample ($n = 5$). $^{*}p < 0.05$ from the dissociated ASC group using the same immunofluorescence.

ASC derived from cell sheets into non-mesenchymal lineages, which may account for the regenerative potential of ASC sheets. However, ASCs with increased plasticity also impose concerns due to unrestricted cell differentiation, so further studies are warranted to clarify the safety issue for clinical use.

5. Conclusions

In the present study, we demonstrated that A2-P-mediated ASC sheets can be effectively fabricated on common tissue culture plates. Abundant deposition of ECM molecules, such as collagen, fibronectin and laminin, was found in ASC sheets. During the ASC sheet formation process, A2-P further upregulated pluripotent genes, including *Oct4*, *Sox2* and *Nanog*, through stimulating collagen synthesis. We showed that ASC sheets exhibited significantly enhanced neurogenic and hepatogenic transdifferentiation capabilities comparing to control ASCs. The regenerative potential of ASC sheets was further demonstrated in a cutaneous wound model of nude mice, and significantly more ASCs differentiating into non-mesenchymal cell lineages were observed in the wound sections. These findings suggested that A2-P-mediated ECM biosynthesis can mimic the *in vivo* physiological environment and enhance the stemness and transdifferentiation capabilities of ASCs. Therefore, A2-P-induced ASC sheet formation may be valuable for many tissue engineering applications.

Acknowledgments

The project was supported by the National Science Council of Taiwan (102-2628-B-002-018), National Taiwan University Hospital (102-S2082, UN101-056), and E-Da Hospital-National Taiwan University Hospital Joint Research Program (102-EDN16). The authors also acknowledge the technical assistance from the staff of the Eighth Core Lab of National Taiwan University Hospital.

Appendix A. Supplementary data

Supplementary data related to this article can be found online at http://dx.doi.org/10.1016/j.biomaterials.2014.01.015.

References

[1] Gimble JM, Guilak F. Differentiation potential of adipose derived adult stem (ADAS) cells. Curr Top Dev Biol 2003;58:137–60.
[2] Aust L, Devlin B, Foster SJ, Halvorsen YD, Hicok K, du Laney T, et al. Yield of human adipose-derived adult stem cells from liposuction aspirates. Cytotherapy 2004;6:7–14.
[3] Fraser JK, Wulur I, Alfonso Z, Hedrick MH. Fat tissue: an underappreciated source of stem cells for biotechnology. Trends Biotechnol 2006;24:150–4.
[4] Guilak F, Lott KE, Awad HA, Cao Q, Hicok KC, Fermor B, et al. Clonal analysis of the differentiation potential of human adipose-derived adult stem cells. J Cell Physiol 2006;206:229–37.

[5] Lin YC, Grahovac T, Oh SJ, Ieraci M, Rubin JP, Marra KG. Evaluation of a multilayer adipose-derived stem cell sheet in a full-thickness wound healing model. Acta Biomater 2013;9:5243–50.
[6] Ng KW, Hutmacher DW. Reduced contraction of skin equivalent engineered using cell sheets cultured in 3D matrices. Biomaterials 2006;27:4591–8.
[7] Badylak SF. The extracellular matrix as a biologic scaffold material. Biomaterials 2007;28:3587–93.
[8] Cheng NC, Estes BT, Young TH, Guilak F. Genipin-crosslinked cartilage-derived matrix as a scaffold for human adipose-derived stem cell chondrogenesis. Tissue Eng Part A 2013;19:484–96.
[9] Obokata H, Yamato M, Tsuneda S, Okano T. Reproducible subcutaneous transplantation of cell sheets into recipient mice. Nat Protoc 2011;6:1053–9.
[10] Wei F, Qu C, Song T, Ding G, Fan Z, Liu D, et al. Vitamin C treatment promotes mesenchymal stem cell sheet formation and tissue regeneration by elevating telomerase activity. J Cell Physiol 2012;227:3216–24.
[11] Trottier V, Marceau-Fortier G, Germain L, Vincent C, Fradette J. IFATS collection: using human adipose-derived stem/stromal cells for the production of new skin substitutes. Stem Cells 2008;26:2713–23.
[12] Hata R, Senoo H. L-ascorbic acid 2-phosphate stimulates collagen accumulation, cell proliferation, and formation of a three-dimensional tissuelike substance by skin fibroblasts. J Cell Physiol 1989;138:8–16.
[13] Kim JE, Jin DH, Lee SD, Hong SW, Shin JS, Lee SK, et al. Vitamin C inhibits p53-induced replicative senescence through suppression of ROS production and p38 MAPK activity. Int J Mol Med 2008;22:651–5.
[14] Taniguchi M, Arai N, Kohno K, Ushio S, Fukuda S. Anti-oxidative and anti-aging activities of 2-O-alpha-glucopyranosyl-L-ascorbic acid on human dermal fibroblasts. Eur J Pharmacol 2012;674:126–31.
[15] Choi KM, Seo YK, Yoon HH, Song KY, Kwon SY, Lee HS, et al. Effect of ascorbic acid on bone marrow-derived mesenchymal stem cell proliferation and differentiation. J Biosci Bioeng 2008;105:586–94.
[16] Esteban MA, Wang T, Qin B, Yang J, Qin D, Cai J, et al. Vitamin C enhances the generation of mouse and human induced pluripotent stem cells. Cell Stem Cell 2010;6:71–9.
[17] Cao N, Liu Z, Chen Z, Wang J, Chen T, Zhao X, et al. Ascorbic acid enhances the cardiac differentiation of induced pluripotent stem cells through promoting the proliferation of cardiac progenitor cells. Cell Res 2012;22:219–36.
[18] Sato H, Takahashi M, Ise H, Yamada A, Hirose S, Tagawa Y, et al. Collagen synthesis is required for ascorbic acid-enhanced differentiation of mouse embryonic stem cells into cardiomyocytes. Biochem Biophys Res Commun 2006;342:107–12.
[19] Potdar PD, D'Souza SB. Ascorbic acid induces in vitro proliferation of human subcutaneous adipose tissue derived mesenchymal stem cells with upregulation of embryonic stem cell pluripotency markers Oct4 and SOX 2. Hum Cell 2010;23:152–5.
[20] Leung PY, Miyashita K, Young M, Tsao CS. Cytotoxic effect of ascorbate and its derivatives on cultured malignant and nonmalignant cell lines. Anticancer Res 1993;13:475–80.
[21] Shima N, Kimoto M, Yamaguchi M, Yamagami S. Increased proliferation and replicative lifespan of isolated human corneal endothelial cells with L-ascorbic acid 2-phosphate. Invest Ophthalmol Vis Sci 2011;52:8711–7.
[22] Takamizawa S, Maehata Y, Imai K, Senoo H, Sato S, Hata R. Effects of ascorbic acid and ascorbic acid 2-phosphate, a long-acting vitamin C derivative, on the proliferation and differentiation of human osteoblast-like cells. Cell Biol Int 2004;28:255–65.
[23] Tsutsumi K, Fujikawa H, Kajikawa T, Takedachi M, Yamamoto T, Murakami S. Effects of L-ascorbic acid 2-phosphate magnesium salt on the properties of human gingival fibroblasts. J Periodontal Res 2012;47:263–71.
[24] Vermette M, Trottier V, Menard V, Saint-Pierre L, Roy A, Fradette J. Production of a new tissue-engineered adipose substitute from human adipose-derived stromal cells. Biomaterials 2007;28:2850–60.
[25] Yeh TS, Dean Fang YH, Lu CH, Chiu SC, Yeh CL, Yen TC, et al. Baculovirus-transduced, VEGF-expressing adipose-derived stem cell sheet for the treatment of myocardium infarction. Biomaterials 2014;35:174–84.
[26] Neo PY, See EY, Toh SL, Goh JC. Temporal profiling of the growth and multilineage potentiality of adipose tissue-derived mesenchymal stem cells cell-sheets. J Tissue Eng Regen Med 2013. http://dx.doi.org/10.1002/term.1776 [Epub ahead of print].
[27] Jang S, Cho HH, Cho YB, Park JS, Jeong HS. Functional neural differentiation of human adipose tissue-derived stem cells using bFGF and forskolin. BMC Cell Biol 2010;11:25.
[28] Coradeghini R, Guida C, Scanarotti C, Sanguineti R, Bassi AM, Parodi A, et al. A comparative study of proliferation and hepatic differentiation of human adipose-derived stem cells. Cells Tissues Organs 2010;191:466–77.
[29] Nambu M, Ishihara M, Nakamura S, Mizuno H, Yanagibayashi S, Kanatani Y, et al. Enhanced healing of mitomycin C-treated wounds in rats using inbred adipose tissue-derived stromal cells within an atelocollagen matrix. Wound Repair Regen 2007;15:505–10.
[30] Bhogal RK, Bona CA. Regulatory effect of extracellular signal-regulated kinases (ERK) on type I collagen synthesis in human dermal fibroblasts stimulated by IL-4 and IL-13. Int Rev Immunol 2008;27:472–96.
[31] Park HJ, Ock SM, Kim HJ, Lee YB, Choi JM, Cho CS, et al. Vitamin C attenuates ERK signalling to inhibit the regulation of collagen production by LL-37 in human dermal fibroblasts. Exp Dermatol 2010;19:e258–64.
[32] Yang J, Yamato M, Shimizu T, Sekine H, Ohashi K, Kanzaki M, et al. Reconstruction of functional tissues with cell sheet engineering. Biomaterials 2007;28:5033–43.
[33] Ho JH, Chen YF, Ma WH, Tseng TC, Chen MH, Lee OK. Cell contact accelerates replicative senescence of human mesenchymal stem cells independent of telomere shortening and p53 activation: roles of Ras and oxidative stress. Cell Transplant 2011;20:1209–20.
[34] Insinga A, Cicalese A, Faretta M, Gallo B, Albano L, Ronzoni S, et al. DNA damage in stem cells activates p21, inhibits p53, and induces symmetric self-renewing divisions. Proc Natl Acad Sci U S A 2013;110:3931–6.
[35] Gimble JM, Bunnell BA, Chiu ES, Guilak F. Concise review: adipose-derived stromal vascular fraction cells and stem cells: let's not get lost in translation. Stem Cells 2011;29:749–54.
[36] Cohen IG, Adashi EY. Human embryonic stem-cell research under siege—battle won but not the war. N Engl J Med 2011;364:e48.
[37] Cheng NC, Wang S, Young TH. The influence of spheroid formation of human adipose-derived stem cells on chitosan films on stemness and differentiation capabilities. Biomaterials 2012;33:1748–58.
[38] Park E, Patel AN. Changes in the expression pattern of mesenchymal and pluripotent markers in human adipose-derived stem cells. Cell Biol Int 2010;34:979–84.
[39] Engler AJ, Sen S, Sweeney HL, Discher DE. Matrix elasticity directs stem cell lineage specification. Cell 2006;126:677–89.
[40] Cheng NC, Estes BT, Awad HA, Guilak F. Chondrogenic differentiation of adipose-derived adult stem cells by a porous scaffold derived from native articular cartilage extracellular matrix. Tissue Eng Part A 2009;15:231–41.
[41] Decaris ML, Mojadedi A, Bhat A, Leach JK. Transferable cell-secreted extracellular matrices enhance osteogenic differentiation. Acta Biomater 2012;8:744–52.
[42] Lin H, Yang G, Tan J, Tuan RS. Influence of decellularized matrix derived from human mesenchymal stem cells on their proliferation, migration and multilineage differentiation potential. Biomaterials 2012;33:4480–9.
[43] Sugii S, Kida Y, Kawamura T, Suzuki J, Vassena R, Yin YQ, et al. Human and mouse adipose-derived cells support feeder-independent induction of pluripotent stem cells. Proc Natl Acad Sci U S A 2010;107:3558–63.
[44] Cheng NC, Chen SY, Li JR, Young TH. Short-term spheroid formation enhances the regenerative capacity of adipose-derived stem cells by promoting stemness, angiogenesis, and chemotaxis. Stem Cells Transl Med 2013;2:584–94.
[45] Rustad KC, Wong VW, Sorkin M, Glotzbach JP, Major MR, Rajadas J, et al. Enhancement of mesenchymal stem cell angiogenic capacity and stemness by a biomimetic hydrogel scaffold. Biomaterials 2012;33:80–90.
[46] Sasaki M, Abe R, Fujita Y, Ando S, Inokuma D, Shimizu H. Mesenchymal stem cells are recruited into wounded skin and contribute to wound repair by transdifferentiation into multiple skin cell type. J Immunol 2008;180:2581–7.
[47] Silva EA, Kim ES, Kong HJ, Mooney DJ. Material-based deployment enhances efficacy of endothelial progenitor cells. Proc Natl Acad Sci U S A 2008;105:14347–52.